LASER INTERFEROMETER GRAVITATIONAL WAVE OBSERVATORY
- LIGO -
CALIFORNIA INSTITUTE OF TECHNOLOGY
MASSACHUSETTS INSTITUTE OF TECHNOLOGY

Technical Note **LIGO-T2000338–v1** 2020/11/04

Minimizing the Effect of Mirror Perturbations on Quantum Decoherence

Mentors: Jonathan Richardson, Rana Adhikari, Annalisa Allocca

California Institute of Technology
LIGO Project, MS 18-34
Pasadena, CA 91125
Phone (626) 395-2129
Fax (626) 304-9834
E-mail: info@ligo.caltech.edu

Massachusetts Institute of Technology
LIGO Project, Room NW22-295
Cambridge, MA 02139
Phone (617) 253-4824
Fax (617) 253-7014
E-mail: info@ligo.mit.edu

LIGO Hanford Observatory
Route 10, Mile Marker 2
Richland, WA 99352
Phone (509) 372-8106
Fax (509) 372-8137
E-mail: info@ligo.caltech.edu

LIGO Livingston Observatory
19100 LIGO Lane
Livingston, LA 70754
Phone (225) 686-3100
Fax (225) 686-7189
E-mail: info@ligo.caltech.edu

http://www.ligo.caltech.edu/

Contents

1 Analytic formalism

1.1 Goal

The aim of the formalism described in the subsequent sections is to calculate the total mode-matching loss (consequently the squeezing loss) in a complex optical system as a function of small perturbations of the mirror positions and curvatures. This is achieved by developing a machinery that can handle arbitrary optical configurations and capture the coupled-cavity interactions in LIGO.

1.2 Optical field vector

We represent the electric field of an optical beam at any point in the system in the Laguerre-Gaussian eigenbasis of the Output Mode Cleaner (OMC). The OMC is the final cavity in the LIGO system and defines an invariant reference basis, since it is not going to be perturbed. In general this vector space is infinite-dimensional, since there are an infinite number of mode orders. However, in this paper we consider only small perturbations in mirror position and radius of curvature from the perfectly mode-matched system. This results in significant transfer of power from the fundamental mode into only the LG_{10} mode [1, 2].

Under this assumption, we consider only a two-dimensional vector space whose basis vectors are the LG_{00} and LG_{10} eigenmodes of the OMC cavity. Using the Dirac notation, we thus represent the electric field at any point as

$$\begin{aligned} |\Psi\rangle &= \begin{pmatrix} \alpha \\ \beta \end{pmatrix} \\ &= \alpha\,|LG_{00}\rangle + \beta\,|LG_{10}\rangle \end{aligned} \tag{1}$$

As the Laguerre-Gauss modes are orthonormal, we have an orthonormal basis, i.e.,

$$\langle LG_{m0}|LG_{n0}\rangle = \delta_{mn} \tag{2}$$

where $m, n \in \{0, 1\}$

1.3 Mode Mixing Matrices

Initially, we start with a purely Gaussian input beam. We now consider that the beam goes through an optical element which may couple it to the LG10 mode. We represent this phenomenon by a 2×2 scattering matrix, say A, such that

$$|\Psi_{\mathrm{out}}\rangle = A \times |\Psi_{\mathrm{in}}\rangle \tag{3}$$

If the beam goes through multiple consecutive elements with the scattering matrices $A_0, A_1, ...A_n$, we have

$$|\Psi_{\mathrm{out}}\rangle = A_n \times ...A_1 \times A_0 \times |\Psi_{\mathrm{in}}\rangle \tag{4}$$

In this way we use this formalism to keep track of the power losses to the first-order mode.

1.3.1 Reflection matrix

The scattering matrix for reflection of a beam from a mirror having amplitude reflectivity coefficient r is given by

$$\mathbf{r} = \begin{pmatrix} r & 0 \\ 0 & r \end{pmatrix} \tag{5}$$

The modified reflection matrix for a radius of curvature perturbation δR in a mirror of radius of curvature R is given by

$$\mathbf{r}' = \mathbf{a}.\mathbf{r} = \begin{pmatrix} r\sqrt{1-a^2} & -\imath ra \\ -\imath ra & r\sqrt{1-a^2} \end{pmatrix} \tag{6}$$

with $a = \frac{\pi\omega^2(z_m)}{2\lambda R^2}\delta R$ where $\omega(z_m)$ is the beam size at the mirror position z_m and λ is the wavelength of the beam. The derivation has been given in Appendix A.1.

1.3.2 Transmission matrix

The scattering matrix for transmission of a beam through a mirror having amplitude transmissivity coefficient t is given by

$$\mathbf{t} = \begin{pmatrix} t & 0 \\ 0 & t \end{pmatrix} \tag{7}$$

1.3.3 Propagation matrix

Let kL be the phase accumulated by a plane-wave upon one-way propagation across a distance or cavity. If this one-way propagation accumulates a phase ϕ_0 in the LG_{00} mode,

$$\phi_0 = kL - \phi_G \tag{8}$$

where ϕ_G is a corrective term known as the Gouy phase. The Gouy phase accounts for the fact that the LG_{00} field propagates at a slower phase velocity than a plane-wave due to its finite transverse localization. Similarly, the correction for mode order LG_{pl} is $(2p + |l|)\phi_G$. Thus if one the one–way propagation accumulates a phase ϕ_1 in the LG_{10} mode, we have $\phi_1 = kL - 3\phi_G = \phi_0 - 2\phi_G$. This phase accumulation during propagation can be represented by the scattering matrix

$$\mathbf{\Phi} = \begin{pmatrix} e^{\imath\phi_0} & 0 \\ 0 & e^{\imath\phi_1} \end{pmatrix} \tag{9}$$

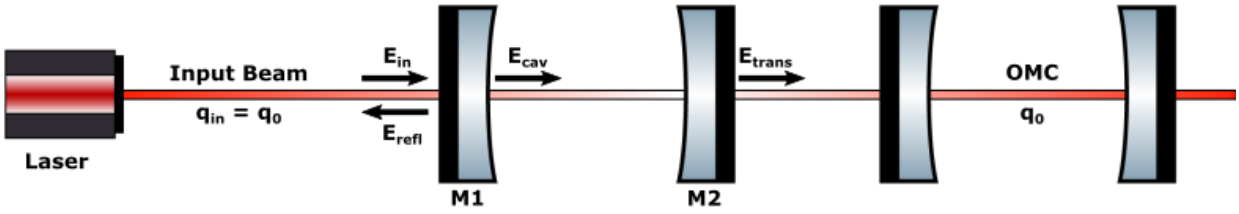

Figure 1: Fabry-Perot cavity before the OMC.

The modified propagation matrix for a position perturbation δz in a mirror of radius of curvature R

$$\mathbf{\Phi'} = \mathbf{b}.\mathbf{\Phi} = \begin{pmatrix} \sqrt{1-b^2}e^{\iota\phi_0} & -be^{\iota\phi_1} \\ -be^{\iota\phi_0} & \sqrt{1-b^2}e^{\iota\phi_1} \end{pmatrix} \tag{10}$$

with $b = \frac{\delta z}{R}$. The derivation has been given in Appendix A.2.

1.4 Total loss

After passing through a complex optical system, let the final beam that reaches the Output Mode Cleaner cavity be $|\Psi_{\text{OMC}}\rangle$. When this beam reaches the OMC cavity, only the LG_{00} mode component couples with the cavity. The LG_{10} mode component is reflected from the cavity and this is the power loss in the system. Thus the total fractional power loss in the system is given by

$$L = \frac{\langle\Psi_{\text{OMC}}|\,|LG_{10}\rangle\,\langle LG_{10}|\,|\Psi_{\text{OMC}}\rangle}{\langle\Psi_{\text{OMC}}|\,|\Psi_{\text{OMC}}\rangle} \tag{11}$$

1.5 Example case for a Fabry-Perot cavity

Consider the setup given in Figure 1, where the input beam with field $|\Psi_{\text{in}}\rangle$, and Fabry-Perot cavity consisting of mirrors M1 and M2 are mode-matched to the OMC cavity. We assume the input beam is

$$|\Psi_{\text{in}}\rangle = \begin{pmatrix} 1 \\ 0 \end{pmatrix} \tag{12}$$

The mirrors M1 and M2 have radii of curvature R_1 and R_2, and reflectivity and transmissivity r_1, r_2 and t_1, t_2 respectively. Let the scattering matrices for reflection by M1, M2 be $\mathbf{r_1}$, $\mathbf{r_2}$

and the scattering matrices for transmission from M1, M2 be $\mathbf{t_1}$, $\mathbf{t_2}$ (given by eqns. 5, 7). if one-way propagation across the Fabry-Perot cavity accumulates a phase ϕ_0 in the LG_{00} mode and ϕ_1 in the LG_{10} mode, this can be represented by the scattering matrix given by eq. 9.

Now for the internal field in the Fabry-Perot cavity, just inside of mirror M1, we have

$$\begin{aligned} |\Psi_{\rm cav}\rangle &= \mathbf{t_1}\,|\Psi_{\rm in}\rangle + \mathbf{r_1}.\mathbf{\Phi}.\mathbf{r_2}.\mathbf{\Phi}\,|\Psi_{\rm cav}\rangle \\ &= \mathbf{t_1}\,|\Psi_{\rm in}\rangle + \mathbf{F_{RT}}\,|\Psi_{\rm cav}\rangle \end{aligned} \tag{13}$$

where

$$\mathbf{F}_{\rm RT} = \mathbf{r_1}.\mathbf{\Phi}.\mathbf{r_2}.\mathbf{\Phi} \tag{14}$$

is the total scattering matrix for a complete round-trip in the Fabry-Perot cavity starting from just inside mirror M1. Thus we have

$$(\mathbf{I} - \mathbf{F}_{\rm RT})\,|\Psi_{\rm cav}\rangle = \mathbf{t_1}\,|\Psi_{\rm in}\rangle \tag{15}$$

$$\implies |\Psi_{\rm cav}\rangle = (\mathbf{I} - \mathbf{F}_{\rm RT})^{-1}\mathbf{t_1}\,|\Psi_{\rm in}\rangle \tag{16}$$

Similarly for the reflected field we have

$$\begin{aligned} |\Psi_{\rm refl}\rangle &= -\mathbf{r_1}\,|\Psi_{\rm in}\rangle + \mathbf{t_1}.\mathbf{\Phi}.\mathbf{r_2}.\mathbf{\Phi}\,|\Psi_{\rm cav}\rangle \\ &= -\mathbf{r_1}\,|\Psi_{\rm in}\rangle + \mathbf{F_E}\,|\Psi_{\rm cav}\rangle \\ &= -\mathbf{r_1}\,|\Psi_{\rm in}\rangle + \mathbf{F_E}(\mathbf{I} - \mathbf{F_{RT}})^{-1}\mathbf{t_1}\,|\Psi_{\rm in}\rangle \\ &= \mathbf{r_{FP}}\,|\Psi_{\rm in}\rangle \end{aligned} \tag{17}$$

where $\mathbf{F_E} = \mathbf{t_1}.\mathbf{\Phi}.\mathbf{r_2}.\mathbf{\Phi}$, and $\mathbf{r_{FP}} = \mathbf{F_E}(\mathbf{I}-\mathbf{F_{RT}})^{-1}\mathbf{t_1} - \mathbf{r_1}$ is the scattering matrix for reflection the Fabry-Perot cavity.

Similarly for the transmitted field we have

$$\begin{aligned} |\Psi_{\rm trans}\rangle &= \mathbf{t_2}.\mathbf{\Phi}\,|\Psi_{\rm cav}\rangle \\ &= \mathbf{t_2}.\mathbf{\Phi}(\mathbf{I} - \mathbf{F_{RT}})^{-1}\mathbf{t_1}\,|\Psi_{\rm in}\rangle \\ &= \mathbf{t_{FP}}\,|\Psi_{\rm in}\rangle \end{aligned} \tag{18}$$

where $\mathbf{t_{FP}} = \mathbf{t_2}.\mathbf{\Phi}(\mathbf{I} - \mathbf{F_{RT}})^{-1}\mathbf{t_1}$ is the scattering matrix for transmittance through the Fabry-Perot cavity. Thus we have effectively reduced the Fabry-Perot cavity to a single mirror M_{FP} with $\mathbf{t} = \mathbf{t_{FP}}$ and $\mathbf{r} = \mathbf{r_{FP}}$ as shown in Figure 2.

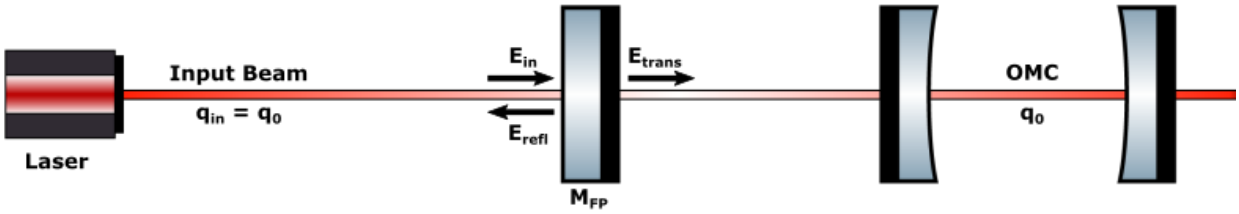

Figure 2: Fabry-Perot cavity before the OMC reduced to a single mirror.

Initially, when the input beam and the two cavities are perfectly mode-matched, we calculate the transmittance matrix by simply substituting eqns. 5, 7, 9, 14. After solving the matrix algebra we get

$$\mathbf{t_{FP}} = \begin{pmatrix} \frac{t_1 t_2 e^{\iota\phi_0}}{1-r_1 r_2 e^{2\iota\phi_0}} & 0 \\ 0 & \frac{t_1 t_2 e^{\iota\phi_1}}{1-r_1 r_2 e^{2\iota\phi_1}} \end{pmatrix} \tag{19}$$

$$\begin{aligned} \implies |\Psi_{\text{trans}}\rangle &= \begin{pmatrix} \frac{t_1 t_2 e^{\iota\phi_0}}{1-r_1 r_2 e^{2\iota\phi_0}} & 0 \\ 0 & \frac{t_1 t_2 e^{\iota\phi_1}}{1-r_1 r_2 e^{2\iota\phi_1}} \end{pmatrix} \begin{pmatrix} 1 \\ 0 \end{pmatrix} \\ &= \frac{t_1 t_2 e^{\iota\phi_0}}{1 - r_1 r_2 e^{2\iota\phi_0}} |LG_{00}\rangle \end{aligned} \tag{20}$$

Thus from eq. 11 we have loss $L = 0$. This is consistent as we have not made any perturbations yet, and so there is no scattering.

1.5.1 Curvature perturbation of the second mirror

We now introduce a radius of curvature perturbation δR in mirror M2 of the Fabry-Perot cavity. Thus from eq. 6 we have with $a = \frac{\pi\omega^2(z)}{2\lambda R_2^2}\delta R$ the scattering matrix for reflection from mirror M2

$$\mathbf{r_2'} = \begin{pmatrix} r_2\sqrt{1-a^2} & -\iota r_2 a \\ -\iota r_2 a & r_2\sqrt{1-a^2} \end{pmatrix} \tag{21}$$

We now repeat the matrix algebra with $\mathbf{F'_{RT}} = \mathbf{r_1}.\mathbf{\Phi}.\mathbf{r_2'}.\mathbf{\Phi}$ and $\mathbf{t'_{FP}} = \mathbf{t_2}.\mathbf{\Phi}(\mathbf{I} - \mathbf{F'_{RT}})^{-1}\mathbf{t_1}$ to get

$$\begin{aligned}\mathbf{t'_{FP}} =& \frac{t_1 t_2}{1 - r_1 r_2 \sqrt{1-a^2}(e^{2\iota\phi_0} + e^{2\iota\phi_1}) + r_1^2 r_2^2 e^{2\iota(\phi_0+\phi_1)}} \\ & \times \begin{pmatrix} e^{\iota\phi_0}(1 - r_1 r_2 \sqrt{1-a^2} e^{2\iota\phi_1}) & -\iota r_1 r_2 a e^{\iota(2\phi_0+\phi_1)} \\ -\iota r_1 r_2 a e^{\iota(\phi_0+2\phi_1)} & e^{\iota\phi_1}(1 - r_1 r_2 \sqrt{1-a^2} e^{2\iota\phi_0}) \end{pmatrix}\end{aligned} \tag{22}$$

$$\begin{aligned}\implies |\Psi'_{\text{trans}}\rangle =& \frac{t_1 t_2}{1 - r_1 r_2 \sqrt{1-a^2}(e^{2\iota\phi_0} + e^{2\iota\phi_1}) + r_1^2 r_2^2 e^{2\iota(\phi_0+\phi_1)}} \\ & \times \begin{pmatrix} e^{\iota\phi_0}(1 - r_1 r_2 \sqrt{1-a^2} e^{2\iota\phi_1}) \\ -\iota r_1 r_2 a e^{\iota(\phi_0+2\phi_1)} \end{pmatrix}\end{aligned} \tag{23}$$

Thus from eq. 11 we have loss

$$L = \frac{r_1^2 r_2^2 a^2}{1 + r_1^2 r_2^2 - 2 r_1 r_2 \cos 2\phi_1 \sqrt{1-a^2}} \tag{24}$$

Assuming $a << 1$, we have $\sqrt{1-a^2} \approx 1$. Substituting in the above equation

$$L = \frac{r_1^2 r_2^2}{1 + r_1^2 r_2^2 - 2 r_1 r_2 \cos 2\phi_1} \left(\frac{\pi \omega^2(z)}{2\lambda R_2^2}\right)^2 \delta R^2 \tag{25}$$

We define the sensitivity to loss as the amount of loss per curvature perturbation δR

$$\left.\frac{\partial L}{\partial(\Delta R)}\right|_{\Delta R = \delta R} = \frac{2 r_1^2 r_2^2}{1 + r_1^2 r_2^2 - 2 r_1 r_2 \cos 2\phi_1} \left(\frac{\pi \omega^2(z)}{2\lambda R_2^2}\right)^2 \delta R \tag{26}$$

We now verify this result using simulations in Finesse. We simulate the set-up given in Fig. 1 with the Fabry-Perot cavity initially mode matched to the OMC. We then plot the power loss percentage at the output of the OMC as a function of the radius of curvature perturbation percentage in mirror 2, keeping all other parameters stable. The results are shown in Fig. 3.

1.5.2 Curvature perturbation of the first mirror

We now introduce a radius of curvature perturbation δR in mirror M1 of the Fabry-Perot cavity. Thus from eq. 6 we have with $a = \frac{\pi \omega^2(z)}{2\lambda R_1^2} \delta R$ the scattering matrix for reflection from mirror M2

$$\mathbf{r'_1} = \begin{pmatrix} r_1 \sqrt{1-a^2} & -\iota r_1 a \\ -\iota r_1 a & r_1 \sqrt{1-a^2} \end{pmatrix} \tag{27}$$

We now repeat the same matrix algebra as in the above section with $\mathbf{F'_{RT}} = \mathbf{r'_1}.\mathbf{\Phi}.\mathbf{r_2}.\mathbf{\Phi}$ and $\mathbf{t'_{FP}} = \mathbf{t_2}.\mathbf{\Phi}(\mathbf{I} - \mathbf{F'_{RT}})^{-1}\mathbf{t_1}$ to get

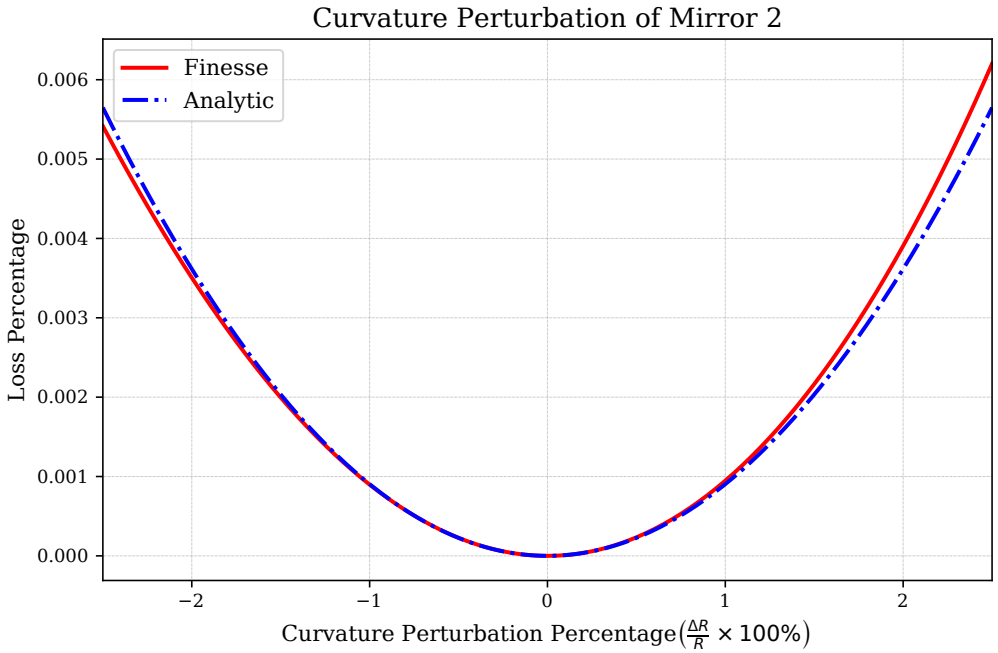

Figure 3: Analytic and simulation results for power loss percentage at output of the OMC cavity as a function of curvature perturbation percentage at mirror 2 of the Fabry-Perot cavity. Initially, the Fabry-Perot cavity is mode-matched to the OMC and we have used cavity parameters: $r_1 = r_2 = 0.9$, $t_1 = t_2 = 0.1$, $R_1 = -17\text{m}$, $R_2 = 20\text{m}$, $L = 10\text{m}$

$$|\Psi'_{\text{trans}}\rangle = \frac{t_1 t_2}{1 - r_1 r_2\sqrt{1-a^2}(e^{2\iota\phi_0} + e^{2\iota\phi_1}) + r_1^2 r_2^2 e^{2\iota(\phi_0+\phi_1)}} \times \begin{pmatrix} e^{\iota\phi_0}(1 - r_1 r_2\sqrt{1-a^2}e^{2\iota\phi_1}) \\ -\iota r_1 r_2 a e^{\iota(2\phi_0+\phi_1)} \end{pmatrix} \tag{28}$$

Thus from eq. 11 we have loss

$$L = \frac{r_1^2 r_2^2 a^2}{1 + r_1^2 r_2^2 - 2r_1 r_2 \cos 2\phi_1\sqrt{1-a^2}} \tag{29}$$

which is the same as for perturbation of the second mirror.

We now verify this result using simulations in Finesse. We simulate the set-up given in Fig. 1 with the Fabry-Perot cavity initially mode matched to the OMC. We then plot the power loss percentage at the output of the OMC as a function of the radius of curvature perturbation percentage in mirror 1, keeping all other parameters stable. The results are shown in Fig. 4.

1.5.3 Position perturbation of the second mirror

We now introduce a perturbation δz in the longitudinal position of mirror M2 of the Fabry-Perot cavity. Thus from eq. 10 we have with $b = \frac{\delta z}{R_2}$ the modified scattering matrix for propagation matrix for the cavity

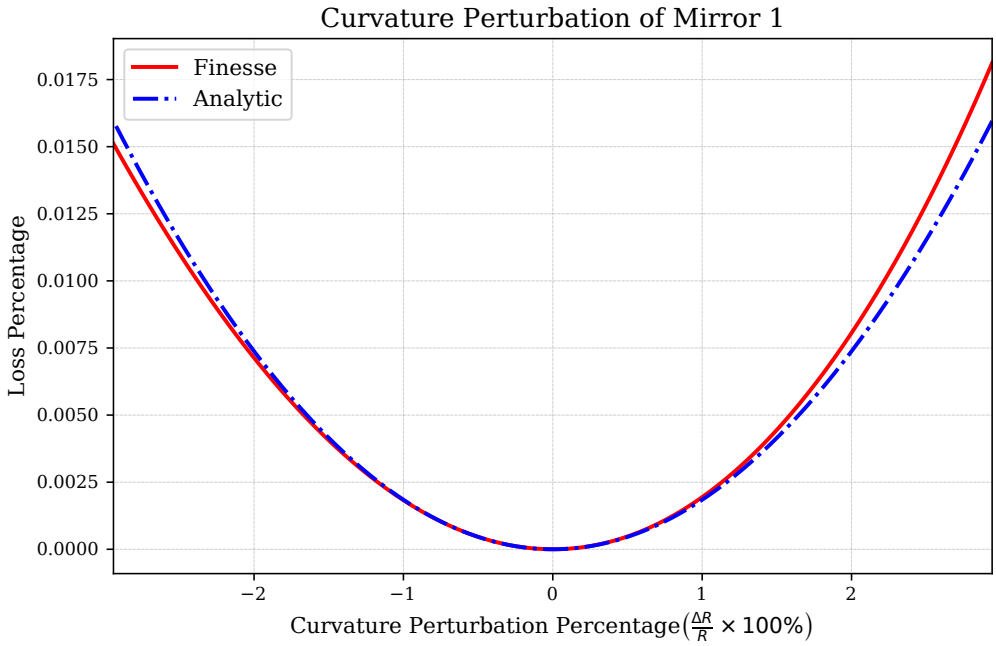

Figure 4: Analytic and simulation results for power loss percentage at output of the OMC cavity as a function of curvature perturbation percentage at mirror 1 of the Fabry-Perot cavity. Initially, the Fabry-Perot cavity is mode-matched to the OMC and we have used cavity parameters: $r_1 = r_2 = 0.9$, $t_1 = t_2 = 0.1$, $R_1 = -17$m, $R_2 = 20$m, $L = 10$m

$$\mathbf{\Phi'} = \begin{pmatrix} \sqrt{1-b^2}e^{\iota\phi_0} & -be^{\iota\phi_1} \\ -be^{\iota\phi_0} & \sqrt{1-b^2}e^{\iota\phi_1} \end{pmatrix} \tag{30}$$

We now repeat the matrix algebra with $\mathbf{F'_{RT}} = \mathbf{r_1}.\mathbf{\Phi'}.\mathbf{r_2}.\mathbf{\Phi'}$ and $\mathbf{t'_{FP}} = \mathbf{t_2}.\mathbf{\Phi'}(\mathbf{I} - \mathbf{F'_{RT}})^{-1}\mathbf{t_1}$ to get

$$\begin{aligned} \mathbf{t'_{FP}} =& \frac{t_1 t_2}{1 - r_1 r_2((1-b^2)e^{2\iota\phi_0} + 2b^2 e^{\iota(\phi_0+\phi_1)} + e^{2\iota\phi_1}(1 - b^2 - (1-2b^2)^2 e^{2\iota\phi_0} r_1 r_2))} \\ & \times \begin{pmatrix} \sqrt{1-b^2}e^{\iota\phi_0}(1-(1-2b^2)e^{2\iota\phi_1} r_1 r_2) & -be^{\iota\phi_0}(1-(1-2b^2)r_1 r_2 e^{\iota(\phi_0+\phi_1)}) \\ -be^{\iota\phi_1}(1-(1-2b^2)r_1 r_2 e^{\iota(\phi_0+\phi_1)}) & \sqrt{1-b^2}e^{\iota\phi_1}(1-(1-2b^2)e^{2\iota\phi_0} r_1 r_2) \end{pmatrix} \end{aligned} \tag{31}$$

Assuming $b << 1$, we approximate up to first order in b

$$\begin{aligned} \mathbf{t'_{FP}} \approx& \frac{t_1 t_2}{1 - r_1 r_2(e^{2\iota\phi_0} + e^{2\iota\phi_1}(1 - e^{2\iota\phi_0} r_1 r_2))} \\ & \times \begin{pmatrix} e^{\iota\phi_0}(1 - e^{2\iota\phi_1} r_1 r_2) & -be^{\iota\phi_0}(1 - e^{\iota(\phi_0+\phi_1)} r_1 r_2) \\ -be^{\iota\phi_1}(1 - e^{\iota(\phi_0+\phi_1)} r_1 r_2) & e^{\iota\phi_1}(1 - e^{2\iota\phi_0} r_1 r_2) \end{pmatrix} \end{aligned} \tag{32}$$

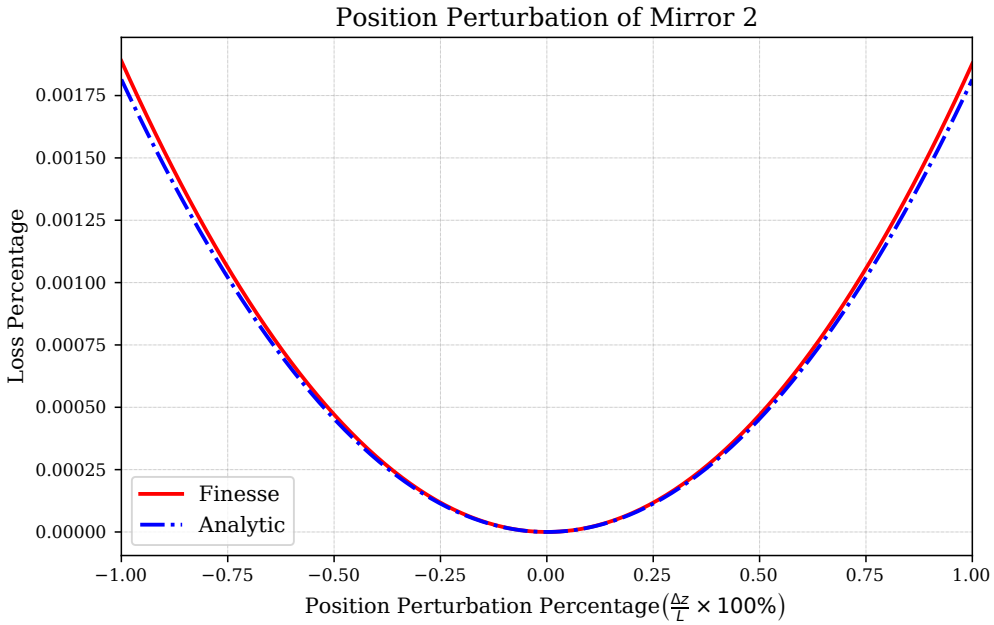

Figure 5: Analytic and simulation results for power loss percentage at output of the OMC cavity as a function of position perturbation percentage at mirror 2 of the Fabry-Perot cavity. Initially, the Fabry-Perot cavity is mode-matched to the OMC and we have used cavity parameters: $r_1 = r_2 = 0.9$, $t_1 = t_2 = 0.1$, $R_1 = -17\text{m}$, $R_2 = 20\text{m}$, $L = 10\text{m}$

$$\implies |\Psi'_{\text{trans}}\rangle = \frac{t_1 t_2}{1 - r_1 r_2 (e^{2\iota\phi_0} + e^{2\iota\phi_1}(1 - e^{2\iota\phi_0} r_1 r_2))} \times \begin{pmatrix} e^{\iota\phi_0}(1 - e^{2\iota\phi_1} r_1 r_2) \\ -b e^{\iota\phi_1}(1 - e^{\iota(\phi_0+\phi_1)} r_1 r_2) \end{pmatrix} \tag{33}$$

Thus from eq. 11 and $b << 1$ we have loss

$$L = \frac{1 + r_1^2 r_2^2 - 2 r_1 r_2 \cos(\phi_0 + \phi_1)}{1 + r_1^2 r_2^2 - 2 r_1 r_2 \cos(2\phi_1)} b^2 \tag{34}$$

We define the sensitivity to loss as the amount of loss per position perturbation δz

$$\left.\frac{\partial L}{\partial(\Delta z)}\right|_{\Delta z = \delta z} = \frac{1 + r_1^2 r_2^2 - 2 r_1 r_2 \cos(\phi_0 + \phi_1)}{1 + r_1^2 r_2^2 - 2 r_1 r_2 \cos(2\phi_1)} \frac{2}{R_2^2} \delta z \tag{35}$$

We now verify this result using simulations in Finesse. We simulate the set-up given in Fig. 1 with the Fabry-Perot cavity initially mode matched to the OMC. We then plot the power loss percentage at the output of the OMC as a function of the position perturbation percentage in mirror 2, keeping all other parameters stable. The results are shown in Fig. 5.

2 Numerical optimisation of design parameters

2.1 Curvature and Position Perturbations in a Fabry-Perot Cavity

Using Finesse we simulate Fig. 1, which represents a Fabry-Perot cavity consisting of mirrors M1 and M2 before the Output Mode Cleaner cavity. In the Fabry Perot cavity as shown, M1 is the input mirror, or the ITM, and M2 is the end mirror, or the ETM. For the purpose of this preliminary analysis, we choose random parameters for the OMC and mode-match the Fabry-Perot cavity parameters accordingly. In this simulation we have used, $r_{ITM} = r_{ETM} = 0.9$, $t_{ITM} = t_{ETM} = 0.1$, $R_{ITM} = -17$m, $R_{ETM} = 20$m, $z_{ITM} = 10$m, $z_{ETM} = 20$m. Thus the length of the Fabry-Perot cavity is $L = 10$m.

2.1.1 Monte Carlo perturbation analysis

We perturb the parameters R_{ITM}, R_{ETM}, z_{ITM}, and z_{ETM} within a $\pm 2\%$ margin around the true values, and generate the density plots for total mode-matching percentage to the unperturbed TEM_{00} mode, as shown in Fig. 6.

We now perform a Monte Carlo optimisation for the same set-up. We optimise the mode-matching percentage to the unperturbed TEM_{00} mode at the output of the Fabry-Perot cavity with respect to the 4 parameters - R_{ITM}, R_{ETM}, z_{ITM}, and z_{ETM}. This optimisation is done within a $\pm 2\%$ perturbation around the true values. The results have been shown in Fig. 7

2.1.2 Particle swarm optimisation of parameters

Particle swarm optimisation (PSO) is a computational method for optimising a given function. We will now use this method to maximise the final mode overlap of the setup while also minimising its sensitivity.

We begin by maximising the mode overlap using PSO. We do so by varying the radii of curvature and positions of the ITM and ETM (R_{ITM}, R_{ETM}, z_{ITM}, and z_{ETM}) and finding the values that maximise the final mode overlap. Using PSO, we don't just restrict ourselves to a $\pm 2\%$ perturbation around the initial true values. Instead we allow a perturbation of ± 1m for z_{ITM} and z_{ETM}, and allow the radii of curvature to take any value such that abs(R) ≥ 0.5m. The corner plot for this optimisation has been shown in Fig. 8. The final values for maximum mode-matching that we get are $R_{ITM} = -17.36$m, $R_{ETM} = 20.09$m, $z_{ITM} = 10.36$m, and $z_{ETM} = 19.97$m. This configuration is one of the many possible configurations for a perfectly mode-matched system within the given perturbations. In the next step we will find the minimally sensitive of all these configurations.

We now use PSO to maximise the final mode overlap of the setup while also minimising its sensitivity. Here we define sensitivity of the setup by the partial derivatives of the final mode overlap with respect to the four parameters (R_{ITM}, R_{ETM}, z_{ITM}, and z_{ETM}). This is defined as the amount of change in the final mode overlap for a small change in these parameters. The function we now wish to maximise is a weighted sum of the mode overlap and the partial derivatives.

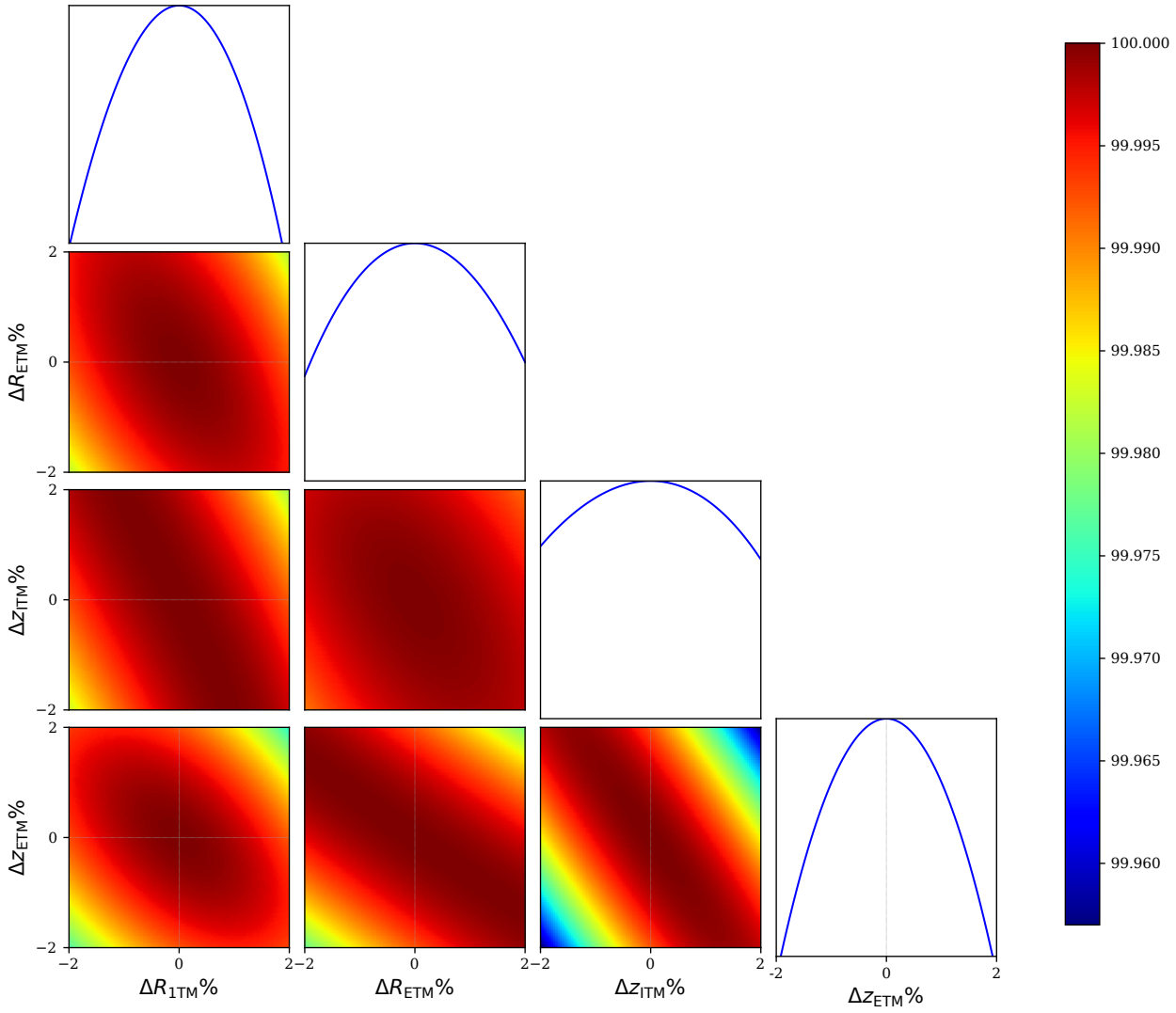

Figure 6: Total mode-matching percentage to the unperturbed TEM_{00} mode at the output of the Fabry-Perot cavity.

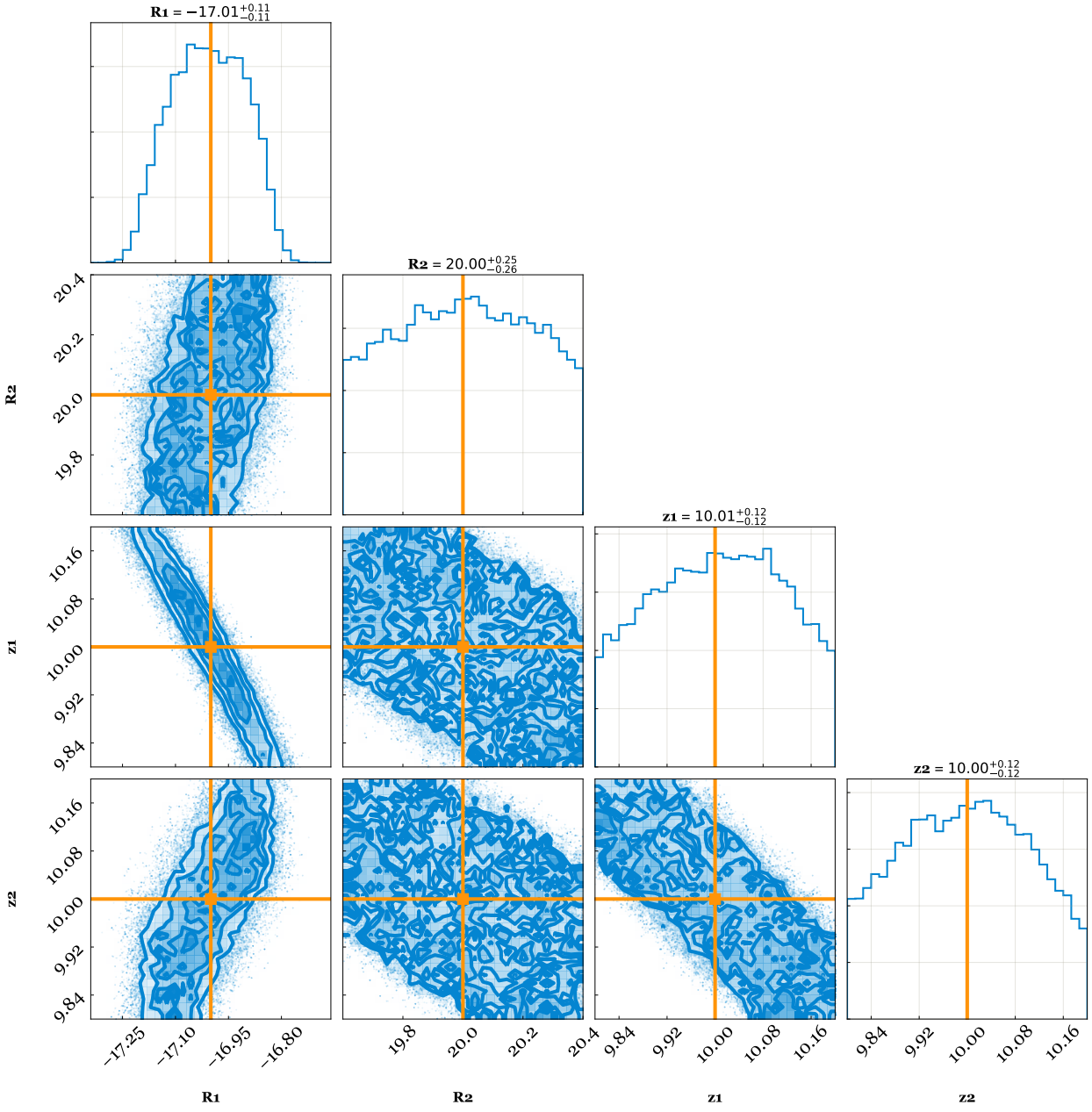

Figure 7: Optimising the total mode-matching percentage at the output of the Fabry-Perot cavity. For the Monte Carlo simulation, we have used: number of walkers = 100, number of steps = 1000.

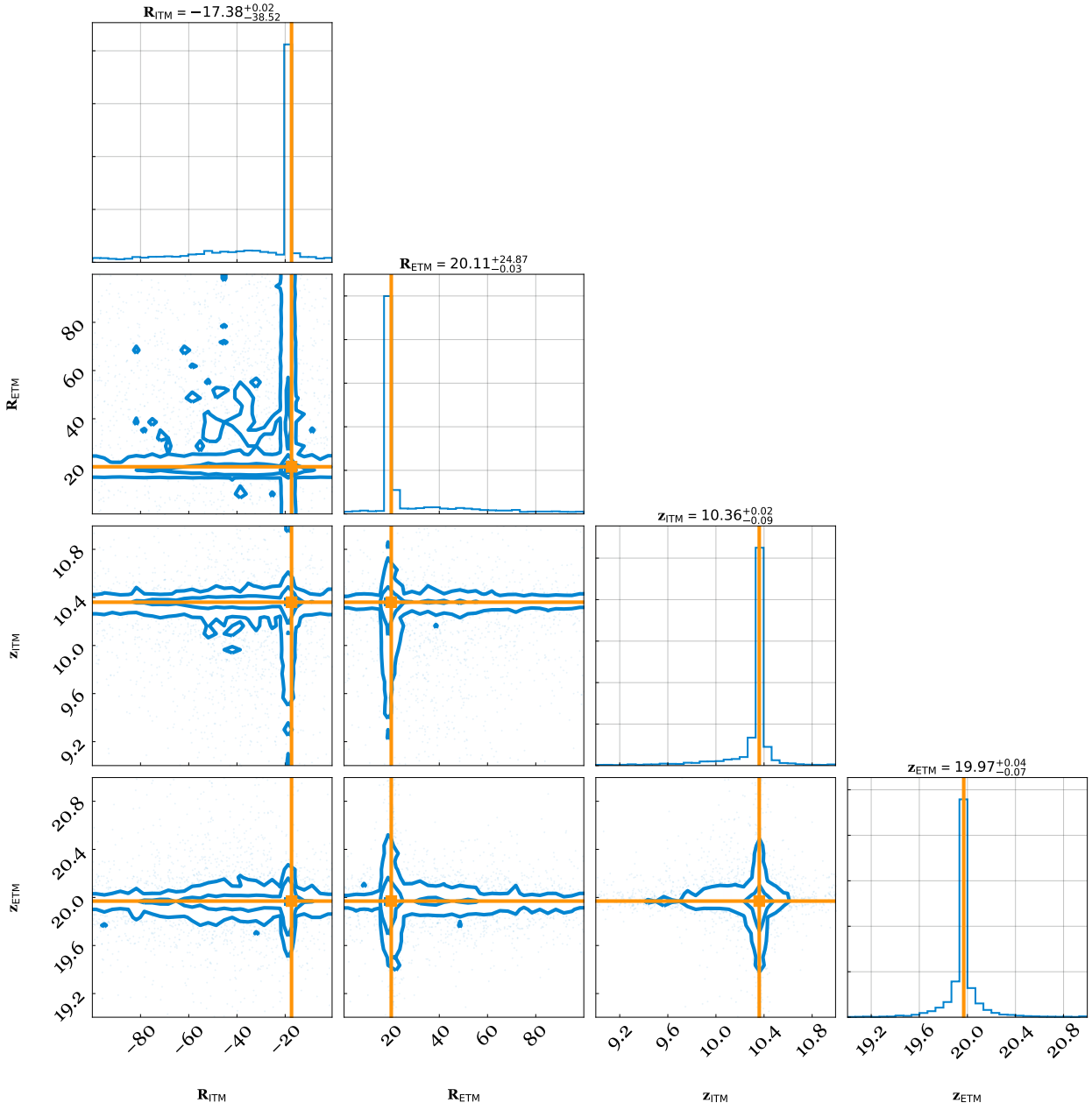

Figure 8: Fabry-Perot before the OMC: Optimising the total mode-matching percentage at the output of the Fabry-Perot cavity. For the particle swarm optimisation, we have used: number of particles = 20, number of steps = 500.

Let the final mode overlap be represented by the function $f(\mathrm{R_{ITM}}, \mathrm{R_{ETM}}, \mathrm{z_{ITM}}, \mathrm{z_{ETM}})$. The function we wish to maximise is then given by

$$F(\mathrm{R_{ITM}}, \mathrm{R_{ETM}}, \mathrm{z_{ITM}}, \mathrm{z_{ETM}}) = \mathrm{af} - \mathrm{b}\left(\left|\frac{\partial \mathrm{f}}{\partial \mathrm{R_{ITM}}}\right| + \left|\frac{\partial \mathrm{f}}{\partial \mathrm{R_{ETM}}}\right| + \left|\frac{\partial \mathrm{f}}{\partial \mathrm{z_{ITM}}}\right| + \left|\frac{\partial \mathrm{f}}{\partial \mathrm{z_{ETM}}}\right|\right) \tag{36}$$

where $a, b > 0$ are weights to ensure mode matching while minimising sensitivity. This means that

$$af >> b\left(\left|\frac{\partial f}{\partial \mathrm{R_{ITM}}}\right| + \left|\frac{\partial f}{\partial \mathrm{R_{ETM}}}\right| + \left|\frac{\partial f}{\partial \mathrm{z_{ITM}}}\right| + \left|\frac{\partial f}{\partial \mathrm{z_{ETM}}}\right|\right) \tag{37}$$

We allow a perturbation of $\pm$1m for $\mathrm{z_{ITM}}$ and $\mathrm{z_{ETM}}$, and allow the radii of curvature to take any value such that abs(R) $\geq$ 0.5m. The corner plot for this this optimisation has been shown in Fig. 9. The final values for minimum sensitivity in a mode-matched system that we get are $\mathrm{R_{ITM}} = -17.59$m, $\mathrm{R_{ETM}} = 21.12$m, $\mathrm{z_{ITM}} = 10.54$m, and $\mathrm{z_{ETM}} = 19.65$m.

2.2 Curvature and Position Perturbations in X-Arm Cavity and Signal Recycling Cavity of the aLIGO System

Using Finesse we simulate Fig. 10, which represents the X-arm cavity and the signal recycling cavity of the aLIGO system. The parameters of the optical setup used for the simulation are the actual aLIGO design parameters. We also place a squeezer vacuum input at the output of the SRC, as shown in the figure.

We once again use particle swarm optimisation to minimise the sensitivity of this setup. This time, we define the sensitivity in terms of output squeezing level instead of mode matching - i.e., we want to minimise the sensitivity to degradation in squeezing level with respect to perturbations in the apparatus. First, we fix the X-arm cavity parameters and minimise the sensitivity with respect to the positions and curvatures of the SRC mirrors (SR3, SR2, SRM). We thus optimise over the six parameters - $\mathrm{R_{SR3}}$, $\mathrm{R_{SR2}}$, $\mathrm{R_{SRM}}$, $\mathrm{L_{SR3}}$, $\mathrm{L_{SR2}}$, $\mathrm{L_{SR1}}$, allowing the radii of curvature to take any value such that abs(R) $\geq$ 1m and the lengths to take any values as long as the total length of the SRC remains constant. We also put conditions to ensure that the beam size at the SRM does not become too large ($\leq$ 1cm) and the interferometer remains locked. During the sensitivity analysis, the input laser beam remains mode-matched to the unperturbed cavity. The results of this optimisation, i.e., the final values for minimum sensitivity in a mode-matched system that we get are given in Table 1.

	$\mathrm{R_{SR3}}$	$\mathrm{R_{SR2}}$	$\mathrm{R_{SRM}}$	$\mathrm{L_{SR3}}$	$\mathrm{L_{SR2}}$	$\mathrm{L_{SR1}}$
aLIGO parameters (m)	35.97	-6.41	-5.69	19.37	15.44	15.76
Optimised parameters (m)	41.14	-20.32	-4.36	14.56	13.69	22.32

Table 1: Optimised SRC parameters for minimum sensitivity to degradation in squeezing level.

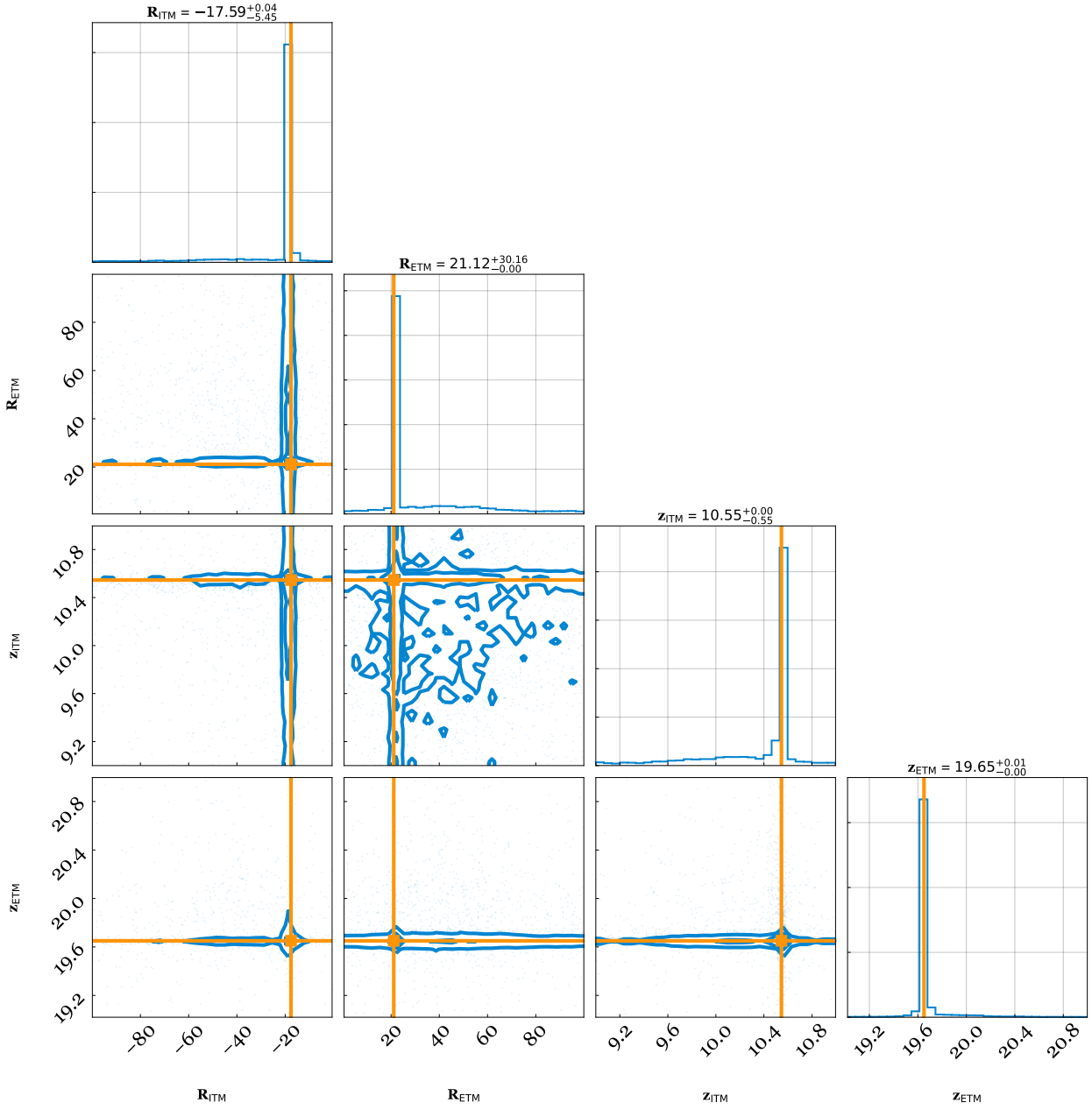

Figure 9: Fabry-Perot before the OMC: Optimising the sensitivity of the setup while ensuring mode-matching. For the particle swarm optimisation, we have used: number of particles = 20, number of steps = 500.

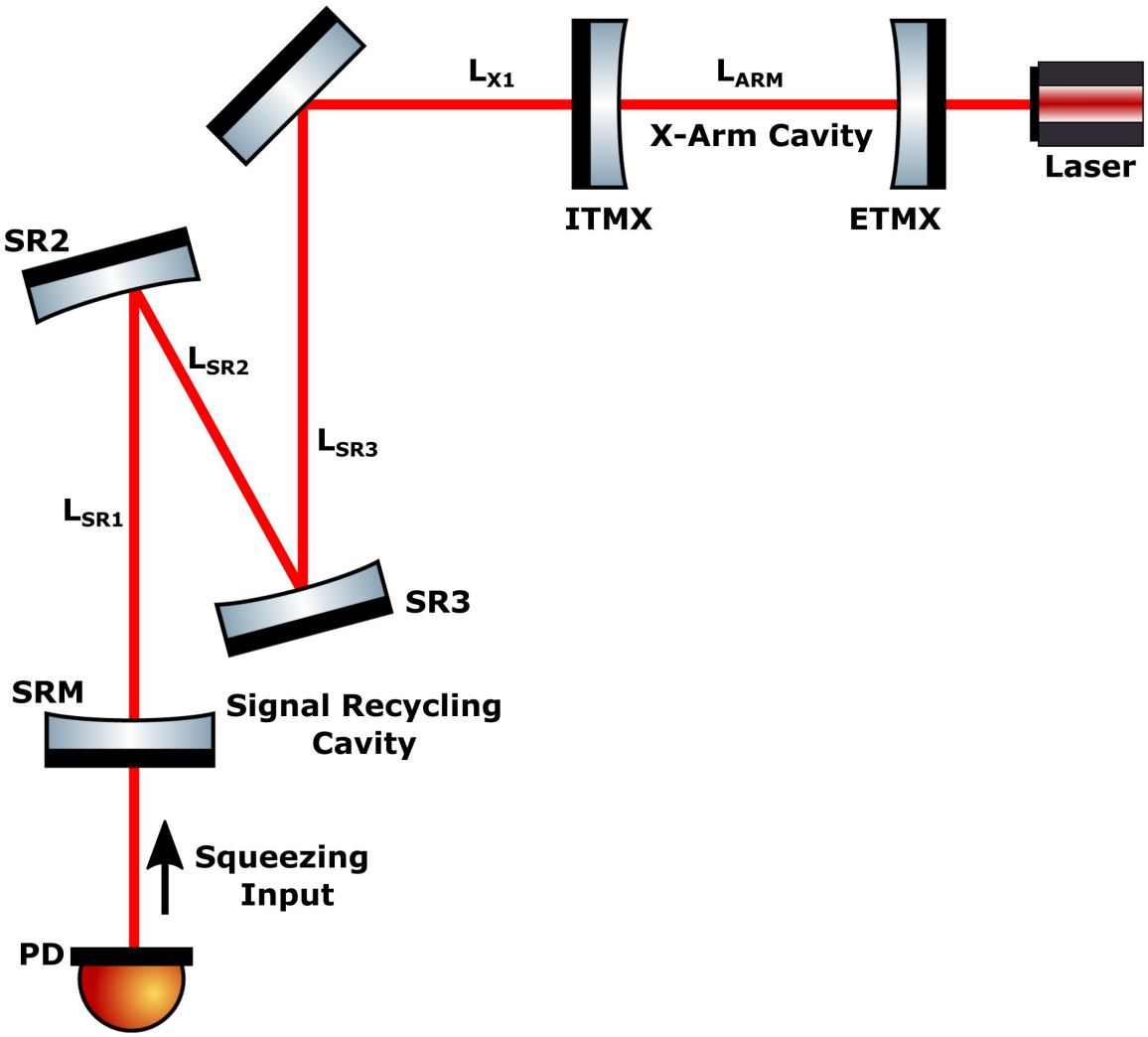

Figure 10: X-arm cavity and the signal recycling cavity of the aLIGO system.

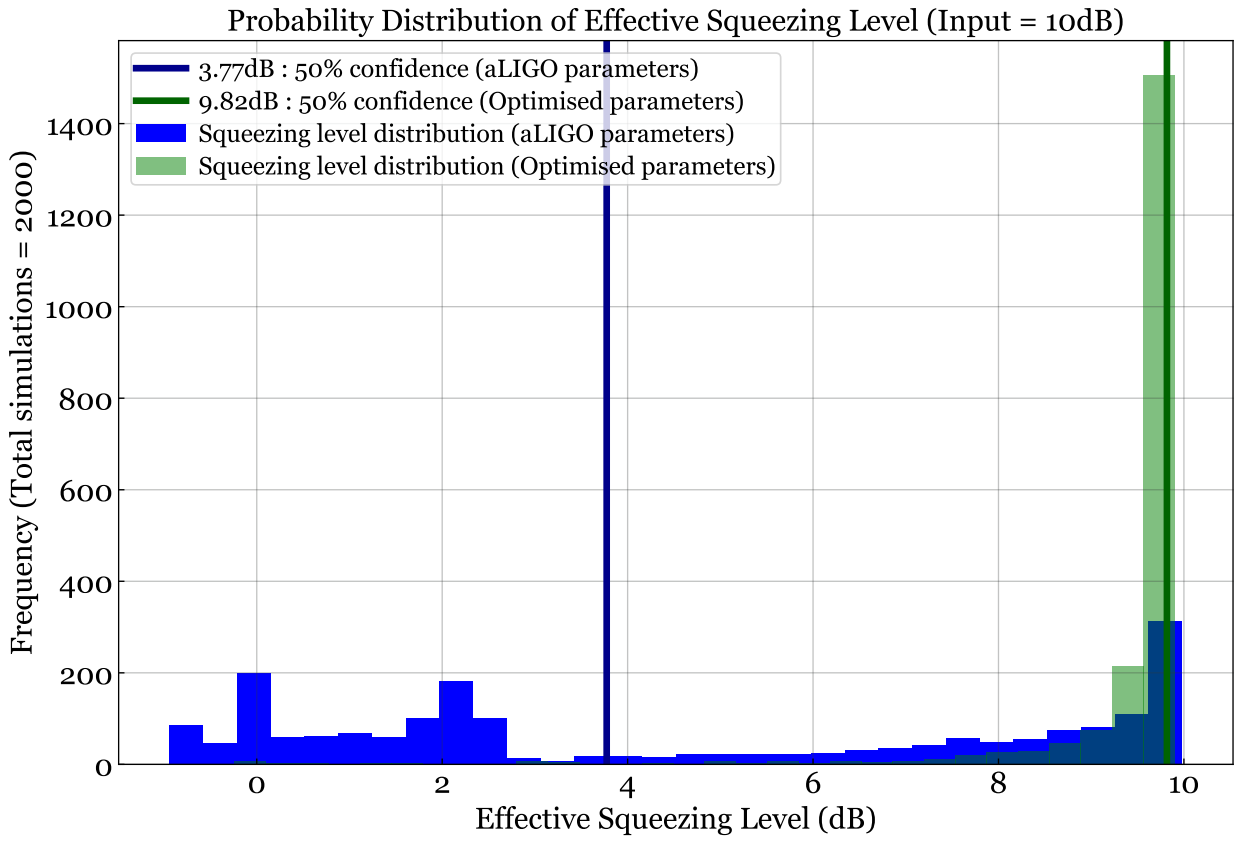

Figure 11: Probability distribution of squeezing levels across 2,000 realisations of the set-up given in Fig. 10 with randomly perturbed SRC mirrors about the aLIGO parameters and optimised parameters given in Table 1.

We now make a quantitative comparison between the squeezing level with the optimised parameters and the actual aLIGO parameters. We quantify the optical setup by the expected level of squeezing at 50% confidence. We first assume typical uncertainties on the curvatures and positions of the SRC mirrors: $\Delta R \sim N(\mu = 0, \sigma = 0.33\%R)$ and $\Delta z \sim N(\mu = 0, \sigma = 3mm)$, where $\sim N$ indicates a normal distribution. We randomly draw a set of ΔR and Δz perturbations for every optical element (SR3, SR2, SRM), and compute the squeezing level for this set of perturbations. During this computation, the input laser beam remains mode-matched to the unperturbed cavity. We repeat this procedure 2,000 times, each time with a different set of randomly-drawn perturbations, and plot the probability distribution of squeezing levels across all 2,000 realizations. We then compute the 50^{th} percentile of the distribution. These results for the aLIGO parameters and the optimised parameters are given in Fig. 11.

We now want to see the effect of perturbations in each individual parameter, to find the parameters to which the design is most sensitive. We thus repeat the same analysis as above for each of the six parameters - R_{SR3}, R_{SR2}, R_{SRM}, L_{SR3}, L_{SR2}, L_{SR1} - perturbing them one at a time. The distributions for the squeezing level are given in Fig. 12.

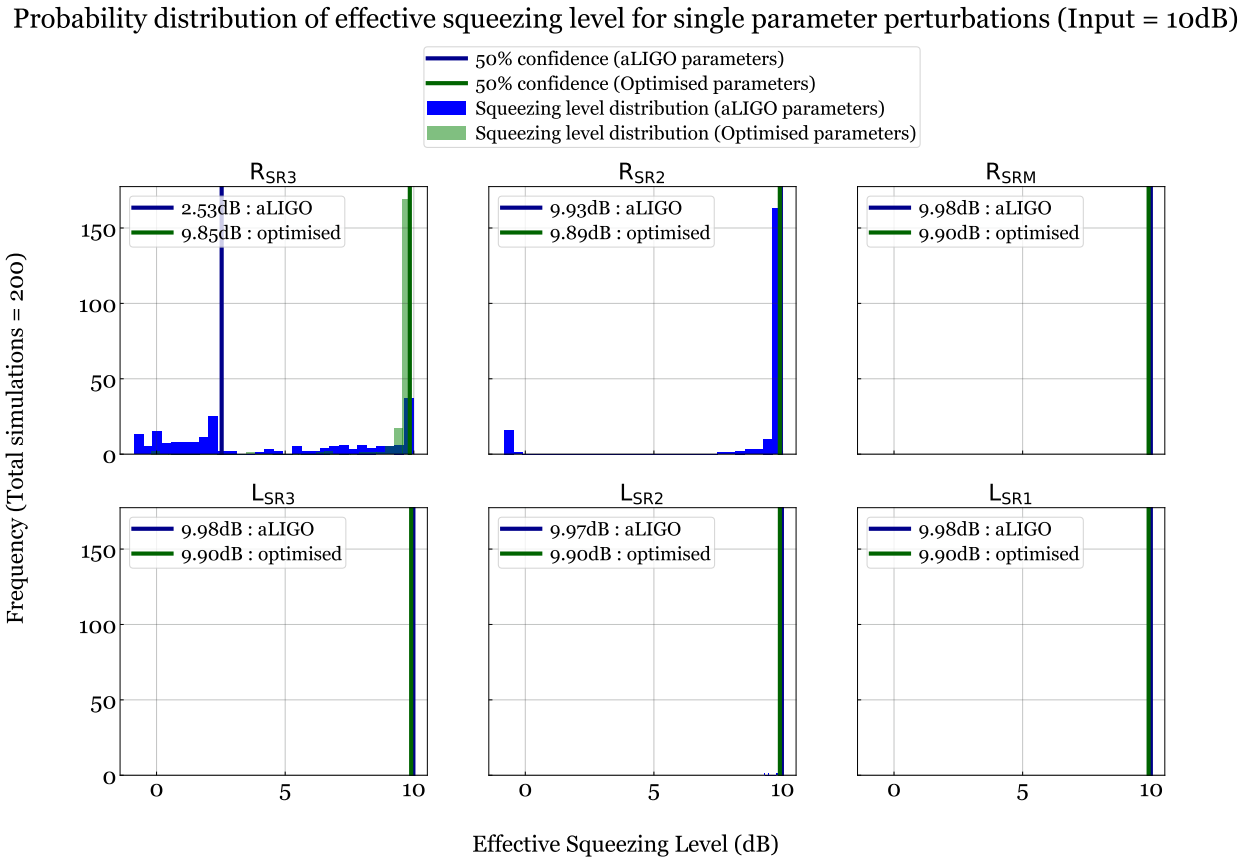

Figure 12: Comparing the probability distributions of squeezing levels perturbing one parameter at a time for the aLIGO parameters and the optimised parameters given in Table 1.

A Derivations of the LG00-LG10 scattering matrices

A.1 Mirror curvature perturbation

Consider the setup given in Figure 13, where the input beam is initially mode-matched to the cavity consisting of mirrors M1 and M2 having radii of curvature R1 and R2 at positions $z = 0$ and $z = z_m$ respectively. At the position of the second mirror ($z = z_m$), we have initially the input beam matched to the LG_{00} radial eigenmode, $U_{00}(r, z_m)$

$$U_{00}(r, z_m) = \sqrt{\frac{2}{\pi}} \frac{1}{\omega(z_m)} \exp(\iota\psi(z_m)) \exp\left[-r^2 \left(\frac{1}{w^2(z_m)} + \iota\frac{\pi}{\lambda R(z_m)}\right)\right] \tag{38}$$

where $\omega(z)$ is the beam size, λ is the wavelength, $R(z)$ is the wavefront curvature, and $\psi(z)$ is the Guoy phase. For the eigenmode, the wavefront curvature at the position of M2 is equal to the mirror curvature R2, i.e., $R(z_m) = R_2$. We now make the radius of curvature perturbation $R_2 \to R_2(1 + \epsilon)$. This will scatter the mode-matched beam into the LG_{10} radial eigenmode of the unperturbed eigenbasis given by

$$U_{10}(r, z_m) = U_{00}(r, z_m) \exp(2\iota\psi(z_m)) \left(1 - \frac{2r^2}{\omega^2(z_m)}\right) \tag{39}$$

Since we are considering the LG_{10} mode at the point of its creation ($z = z_m$), i.e., no propagation has occurred yet, the accumulated phase lag is zero and we have

$$U_{10}(r, z_m) = U_{00}(r, z_m) \left(1 - \frac{2r^2}{\omega^2(z_m)}\right) \tag{40}$$

Now the new eigenmode of the perturbed cavity at $z = z_m$ is given by

$$\begin{aligned} U'_{00}(r, z_m) &= \sqrt{\frac{2}{\pi}} \frac{1}{\omega(z_m)} \exp(\iota\psi(z_m)) \exp\left[-r^2 \left(\frac{1}{w^2(z_m)} + \iota\frac{\pi}{\lambda R_2(1+\epsilon)}\right)\right] \\ &\approx \sqrt{\frac{2}{\pi}} \frac{1}{\omega(z_m)} \exp(\iota\psi(z_m)) \exp\left[-r^2 \left(\frac{1}{w^2(z_m)} + \iota\frac{\pi}{\lambda R_2}\right)\right] \left(1 + \iota\frac{\pi r^2 \epsilon}{\lambda R_2}\right) \end{aligned} \tag{41}$$

for $\epsilon << 1$ upto first-order. Now rearranging the perturbed eigenmode to express it in terms of the unperturbed eigenbasis we have from eqns. 38 and 40

$$U'_{00}(r, z_m) = (1 + \iota a) U_{00}(r, z_m) - \iota a U_{10}(r, z_m) \tag{42}$$

where

$$a = \frac{\pi\omega^2(z_m)}{2\lambda R_2^2} \delta R \tag{43}$$

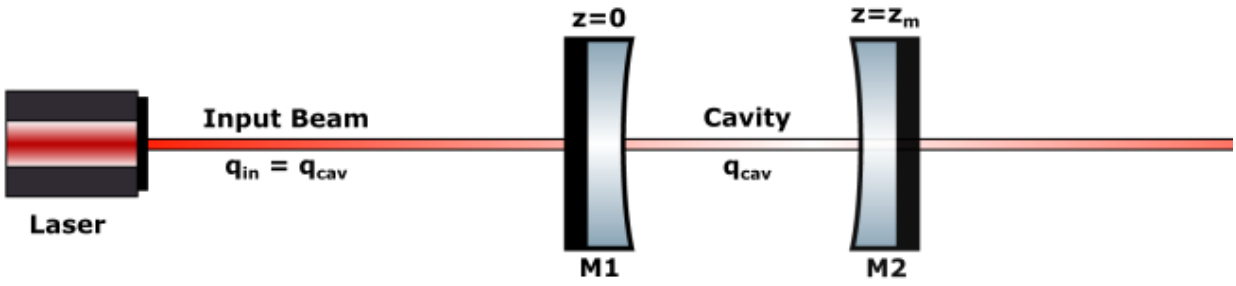

Figure 13: Mirror curvature perturbation.

with $\epsilon = \frac{\delta R}{R}$. As $\epsilon << 1$, we have $1 + \imath a \approx 1$ and hence

$$U'_{00}(r, z_m) = U_{00}(r, z_m) - \imath a U_{10}(r, z_m) \tag{44}$$

Thus at this point, we have scattering of the input beam into the LG_{10} mode. In the unperturbed eigenbasis (eigenbasis of the input beam), we can now represent this by the scattering matrix

$$\mathbf{a} = \begin{pmatrix} \sqrt{1-a^2} & -\imath a \\ -\imath a & \sqrt{1-a^2} \end{pmatrix} \tag{45}$$

Here the first column of the matrix represents the scattering from the LG_{00} mode to the LG_{00} and LG_{10} modes. The second column represents the scattering from the LG_{10} mode to the LG_{00} and LG_{10} modes, since there is also a transfer back of power from the LG_{10} mode. The reason for this is explained in Vajente (2014): The amount of scattering for the cases $LG_{00} \rightarrow LG_{00}, LG_{10}$ and $LG_{10} \rightarrow LG_{10}, LG_{00}$ is determined by the mode-overlap integrals,

$$\text{OL} = \int\int U'_{00}(r, z_m) U_{10}(r, z_m)\, dx\, dy \tag{46}$$

and

$$\text{OL} = \int\int U'_{10}(r, z_m) U_{00}(r, z_m)\, dx\, dy \tag{47}$$

which are identical [3]. We have explicitly derived the $LG_{00} \rightarrow LG_{00}, LG_{10}$ case, and we thus assume equal amplitude for the opposite case.

Hence we now have the modified reflection matrix for a radius of curvature perturbation δR in a mirror of radius of curvature R

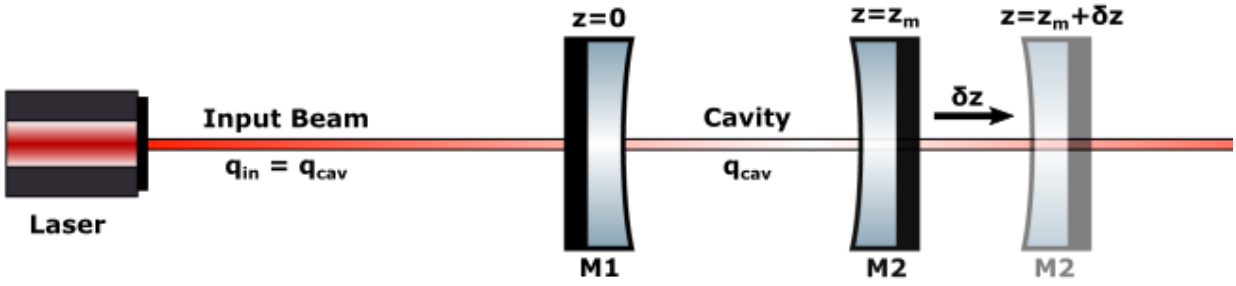

Figure 14: Mirror position perturbation.

$$\mathbf{r}' = \mathbf{a}.\mathbf{r} = \begin{pmatrix} r\sqrt{1-a^2} & -\imath r a \\ -\imath r a & r\sqrt{1-a^2} \end{pmatrix} \tag{48}$$

with $a = \frac{\pi\omega^2(z_m)}{2\lambda R^2}\delta R$

A.2 Mirror position perturbation

Consider the setup given in Figure 14, where the input beam is initially mode-matched to the cavity consisting of mirrors M1 and M2 having radii of curvature R1 and R2 at positions $z = 0$ and $z = z_m$ respectively. At the position of the second mirror ($z = z_m$), we have initially the input beam matched to the LG_{00} radial eigenmode, $U_{00}(r, z_m)$, given by eq. 38. For the eigenmode, the wavefront curvature at the position of M2 is equal to the mirror curvature R2, i.e., $R(z_m) = R_2$.

We now make a perturbation to the second mirror position $z_m \to z_m + \delta z$. This will scatter the mode-matched beam into the LG_{10} radial eigenmode of the unperturbed eigenbasis given by eq. 40

Now the new eigenmode of the perturbed cavity at the new position of the second mirror, $z = z_m + \delta z$ is given by

$$\begin{aligned} U'_{00}(r, z_m + \delta z) &= \sqrt{\frac{2}{\pi}}\frac{1}{\omega(z_m+\delta z)}\exp(\imath\psi(z_m+\delta z))\exp\left[-r^2\left(\frac{1}{w^2(z_m+\delta z)} + \imath\frac{\pi}{\lambda R(z_m+\delta z)}\right)\right] \\ &= \sqrt{\frac{2}{\pi}}\frac{1}{\omega(z_m+\delta z)}\exp(\imath\psi(z_m+\delta z))\exp\left[-r^2\left(\frac{1}{w^2(z_m+\delta z)} + \imath\frac{\pi}{\lambda R_2}\right)\right] \end{aligned} \tag{49}$$

since M2 has now been moved to $z_m + \delta z$ and hence for the perturbed cavity eigenmode, $R(z_m + \delta z) = R_2$.

The beam size at the new mirror location is

$$\begin{aligned}\omega(z_m + \delta z) &= \omega_0\sqrt{1 + \left(\frac{z_m - z_0 + \delta z}{z_R}\right)^2} \\ &\approx \omega(z_m)\left(1 + \frac{z_m - z_0}{(z_m - z_0)^2 + z_R^2}\delta z\right)\end{aligned} \tag{50}$$

assuming $\delta z << z_R$ and taking upto first order in δz, where ω_0 is the beam waist and z_R is the Rayleigh range.

From [4] we have

$$z_R = \frac{\pi\omega_0^2}{\lambda} \tag{51}$$

$$\omega_0^2 = \frac{\omega^2(z_m)}{1 + \left(\frac{\pi\omega^2(z_m)}{\lambda R_2}\right)^2} \tag{52}$$

$$z_m - z_0 = \frac{R_2}{1 + \left(\frac{\lambda R_2}{\pi\omega^2(z_m)}\right)^2} \tag{53}$$

Now let $\alpha = \frac{\lambda R_2}{\pi\omega^2(z_m)}$. Then we have

$$z_m - z_0 = \frac{R_2}{1 + \alpha^2} \tag{54}$$

and

$$z_R = \alpha(z_m - z_0) \tag{55}$$

$$\implies \frac{z_m - z_0}{(z_m - z_0)^2 + z_R^2} = \frac{1}{R_2} \tag{56}$$

Thus we have

$$\omega(z_m + \delta z) = \omega(z_m)\left(1 + \frac{\delta z}{R_2}\right) \tag{57}$$

Now we calculate the Guoy phase at the new mirror location

$$\begin{aligned}\psi(z_m+\delta z) &= \arctan\left(\frac{z_m-z_0+\delta z}{z_R}\right)\\ &\approx \arctan\left(\frac{z_m-z_0}{z_R}\right)+\frac{z_R\,\delta z}{(z_m-z_0)^2+z_R^2}\\ &= \psi(z_m)+\frac{\lambda\,\delta z}{\pi\omega^2(z_m)}\\ &\approx \psi(z_m)\end{aligned} \tag{58}$$

using $\lambda << \omega(z_m)$ and $\delta z \sim \omega(z_m)$.

Substituting eqns. 57, 58 in eq. 49, we rewrite the new eigenmode of the perturbed cavity at $z = z_m + \delta z$ as

$$\begin{aligned}U'_{00}(r, z_m+\delta z_m) &= \sqrt{\frac{2}{\pi}}\frac{1}{\omega(z_m)}\left(1+\frac{\delta z}{R_2}\right)^{-1}\exp(\iota\psi(z_m))\exp\left[-r^2\left(\frac{1}{w^2(z_m)}\left(1+\frac{\delta z}{R_2}\right)^{-2}+\iota\frac{\pi}{\lambda R_2}\right)\right]\\ &\approx U_{00}(r,z_m)\left[1-\frac{\delta z}{R_2}\left(1-\frac{2r^2}{\omega^2(z_m)}\right)\right]\end{aligned} \tag{59}$$

using $\delta z << R_2$ and calculating upto first order in δz. Thus rearranging the perturbed eigenmode to express it in terms of the unperturbed eigenbasis we have

$$U'_{00}(r, z_m+\delta z_m) = U_{00}(r,z_m) - \frac{\delta z}{R_2}U_{10}(r,z_m) \tag{60}$$

Thus at this point, we have scattering of the input beam into the LG_{10} mode. In the unperturbed eigenbasis (eigenbasis of the input beam), we can now represent this by the scattering matrix

$$\mathbf{b} = \begin{pmatrix}\sqrt{1-b^2} & -b\\ -b & \sqrt{1-b^2}\end{pmatrix} \tag{61}$$

where $b = \frac{\delta z}{R_2}$. Hence we now have the modified propagation matrix for a position perturbation δz in a mirror of radius of curvature R

$$\mathbf{\Phi'} = \mathbf{b}.\mathbf{\Phi} = \begin{pmatrix}\sqrt{1-b^2}e^{\iota\phi_0} & -be^{\iota\phi_1}\\ -be^{\iota\phi_0} & \sqrt{1-b^2}e^{\iota\phi_1}\end{pmatrix} \tag{62}$$

with $b = \frac{\delta z}{R}$

References

[1] D. Z. Anderson, "Alignment of resonant optical cavities," *Appl. Opt.*, vol. 23, pp. 2944–2949, Sep 1984.

[2] A. Perreca, A. F. Brooks, J. W. Richardson, D. Töyrä, and R. Smith, "Analysis and visualization of the output mode-matching requirements for squeezing in Advanced LIGO and future gravitational wave detectors," *Phys. Rev. D*, vol. 101, p. 102005, May 2020.

[3] G. Vajente, "In situ correction of mirror surface to reduce round-trip losses in Fabry-Perot cavities," *Appl. Opt.*, vol. 53, pp. 1459–1465, Mar 2014.

[4] H. Kogelnik and T. Li, "Laser beams and resonators," *Appl. Opt.*, vol. 5, pp. 1550–1567, Oct 1966.